

Galaxies with Unusually High Abundances of Molecular Hydrogen

A. V. Kasparova*

Sternberg Astronomical Institute.

A. V. Zasov†

Sternberg Astronomical Institute.

A sample of 66 galaxies from the catalog of Bettoni et al. (CISM) with anomalously high molecular-to-atomic hydrogen mass ratios ($M_{mol}/M_{HI} > 2$) is considered. The sample galaxies do not differ systematically from other galaxies in the catalog with the same morphological types, in terms of their photometric parameters, rotational velocities, dust contents, or the total mass of gas in comparison with galaxies of similar linear sizes and disk angular momentum. This suggests that the overabundance of H_2 is due to transition of $HI \rightarrow H_2$. Galaxies with bars and active nuclei are found more frequently among galaxies which have M_{mol} estimates in CISM. In a small fraction of galaxies, high M_{mol}/M_{HI} ratios are caused by the overestimation of M_{mol} due to a low conversion factor for the translation of CO -line intensities into the number of H_2 molecules along the line of sight. It is argued that the "molecularization" of the bulk of the gas mass could be due 1) to the concentration of gas in the inner regions of the galactic disks, resulting to a high gas pressure and 2) to relatively low star-formation rate per unit mass of molecular gas which indeed takes place in galaxies with high M_{mol}/M_{HI} ratios.

Astronomy Reports, 2006, Vol. 50, No. 8, p. 626–637.

1. INTRODUCTION

The densest and coolest component of the interstellar medium — molecular gas — is observed in all types of disk galaxies. In many cases, a mass of molecular gas inside galactic disks is comparable to a mass of neutral hydrogen (HI). The amount and spatial density of molecular gas reflects the specific properties of the evolution of the interstellar medium in galactic disks. The most massive gaseous formations — giant molecular clouds, which affect the dynamical evolution of the disk,— are associated with molecular gas. However, more importantly, the mass and density of the molecular gas determine the star-formation rate and star-formation efficiency in galactic disks.

Despite the crucial role that molecular gas plays in galaxies, the factors determining its abundance relative to neutral gas remain poorly known. Most information on interstellar molecular gas has been obtained from measurements of CO -line intensities — CO has a very low excitation temperature. The conversion of the CO -line luminosity into the total mass of gas is a separate problem. For galaxies with normal heavy-element abundances the conversion factor connecting the CO -line intensity with the number of H_2 molecules along the line of sight, $X = N(H_2)/I_{CO}$, is usually set equal to $(2 - 3) \cdot 10^{20} \text{ mol}/(K \cdot km/s)$, however, the universality of this parameter remains a topic of discussion. Adopting a constant X value is, of course, a simplification, especially when galaxies with strongly differing mass, gas density, or star-

formation intensity are compared. Various methods for measuring X and the dependence of X on the galactic luminosity show appreciable scatter, together with a systematic increase in X with decreasing luminosity (mass) of the galaxy and decreasing heavy-element abundance ([1], [2]). The conversion factors for dwarf galaxies and giant luminous galaxies may differ by an order of magnitude. We also expect X to be smaller for dense circumnuclear disks, where the molecular gas seems to be contained in both clouds and the diffuse intercloud medium ([3], [4]).

Various authors ([5], [6], [7]) have analyzed the conditions for molecular-to-atomic, $M_{mol} \rightarrow M_{HI}$, transformations and vice-versa (see also references in these papers). The rate at which molecules are formed depends on both the density (or pressure) of a gas and on the density of UV flux, which destroys molecules. According to Elmegreen ([6]), the M_{mol}/M_{HI} ratio is proportional to $P^{2.2}/j$, where P is the gas pressure and j is the UV flux density. The gas compression in shocks can also play an important role in the "molecularization" of hydrogen [8].

Since the gas pressure depends both on its surface density and on the volume density of the stellar disk, it decreases rapidly with galactocentric distance. Indeed, the azimuthally averaged density ratio M_{mol}/M_{HI} follows the pressure in such a way that the contribution of M_{mol} to the total mass of gas becomes small at a periphery of the galaxy [7].

Available estimates show that the integrated ratio M_{mol}/M_{HI} is appreciably lower than unity for most spiral galaxies. According to Casoli et al. [9], M_{mol}/M_{HI} is, on the average, close to 0.2. Boselli et al. [1] found the average molecular-to-atomic gas mass ratio to be $M_{mol}/M_{HI} = 0.14$

* akasparova@yandex.ru

† zasov@sai.msu.ru

for a sample of 266 galaxies. However, some spiral galaxies are known to have anomalously high M_{mol}/M_{HI} values, exceeding two or even three (an order of magnitude higher than the average value). Our aim here is to analyze the specific features of such galaxies with a predominance of molecular gas and possible factors that could lead to such high M_{mol}/M_{HI} estimates.

As our initial data, we used "A new catalogue of ISM content of normal galaxies" (CISM) of Bettoni et al. [10]. This catalog contains interstellar-medium data for almost two thousand "normal" galaxies, more than 300 of which have estimates for their molecular-gas mass. Normal galaxies are considered to be those that display no morphological distortion (such as tidal tails or bridges) or strong perturbations of their circular velocities, although several galaxies among those included in the catalog can, nevertheless, be considered to be interacting galaxies (see below). The molecular-gas mass estimate is based on the adopted value of $X = 2.3 \cdot 10^{20} \text{ mol}/K \cdot km/s$, taken to be the same for all galaxies.

2. MAIN PROPERTIES OF GALAXIES WITH A PREDOMINANCE OF H_2

2.1. The Galaxy Sample

We selected a total of 66 objects with anomalously high ratios $M_{mol}/M_{HI} > 2$ from the CISM catalog of Bettoni et al. [10]. Forty-five of these galaxies have $M_{mol}/M_{HI} > 3$. Table 3 gives the main properties of these sample galaxies. We adopted data on the interstellar medium from CISM; photometric and kinematic properties from the HYPERLEDA [11] database, and the photometric scale in accordance with the catalog of Baggett et al. [12]. The columns of the table give: a running number for the galaxy, its name, morphological type (as a number), heliocentric distance (in Mpc), radial photometric scale length (in kpc), B -band luminosity (in solar luminosities), photometric diameter D_{25} (in kpc), logarithm of the dust mass (in solar units), logarithm of the HI mass (in solar units), logarithm of the mass of molecular gas (in solar units), logarithm of the rotational velocity derived from the widths of HI (in km/s), and corrected $U-B$ and $B-V$ color indices. The last column ("Remarks") shows the presence of a bar (B), membership in the Virgo or Coma clusters (V or C), and signs of interaction (VV number according to Vorontsov-Velyaminov).

Figure 1 compares the galaxies in our sample with the CISM galaxies with known molecular-gas contents (below, we will consider only this part of all CISM catalog) in terms of their morphological types, surface brightnesses SB (within the isophotal diameter D_{25}) relative to the av-

TABLE 1: Mean values of some parameters for galaxies of the CISM catalog (sample 1) and for sample galaxies with $M_{mol}/M_{HI} > 2$ (sample 2), with the standard deviations (STD) and the statistical probability of the absence of differences between the two samples (p).

Sample	Mean	STD	p, %
Morphological type			
1	2.80	3.06	95.00
2	2.24	2.24	
Magnitude			
1	-20.75	1.37	99.00
2	-21.06	1.16	
$\log V_{rot}$			
1	2.19	0.21	95.00
2	2.23	0.20	
$\log(M_{dust}/M_{gas})$			
1	-3.38	0.39	99.95
2	-3.21	0.36	

erage surface brightness $\langle SB \rangle$ for CISM galaxies of the same type, absolute B-band magnitude M , and rotational velocity V_{rot} derived from the HI line widths. These distributions show that galaxies with high M_{mol}/M_{HI} ratios are mostly Sa — Sbc galaxies ($t = 1 - 4$), with virtually no late-type galaxies among them. Note that allowing for the luminosity dependence of the conversion factor does not affect the conclusion that galaxies with late morphological types have lower M_{mol}/M_{HI} ratios [13].

The galaxies of our sample are essentially indistinguishable from the other CISM galaxies in terms of the brightness of their stellar disks and their luminosities, although the mean value for M is shifted somewhat toward higher luminosities. The rotational velocities V_{rot} for the sample galaxies and for all the CISM galaxies with available M_{mol} estimates have more or less the same distributions, ranging from 50 to 400 km/s. Table 1 gives the numerical results of these comparisons: the mean values and standard deviations of the quantities compared, and the probability that the difference between the means of the two samples is of random nature. We conclude that the objects in our sample do not differ strongly from the other galaxies in terms of the parameters described above.

Note that galaxies with optical bars make up a significant fraction of galaxies with measured molecular-gas masses (Table 2). Whereas barred galaxies account for about one-third of all the CISM galaxies, they comprise one-half of all galaxies with available molecular-gas mass estimates (which evidently bias to objects with high H_2 abundances). The latter is also true for the galaxies in our sample with $M_{mol}/M_{HI} > 2$. It follows from Table 2 that this sample is characterized by

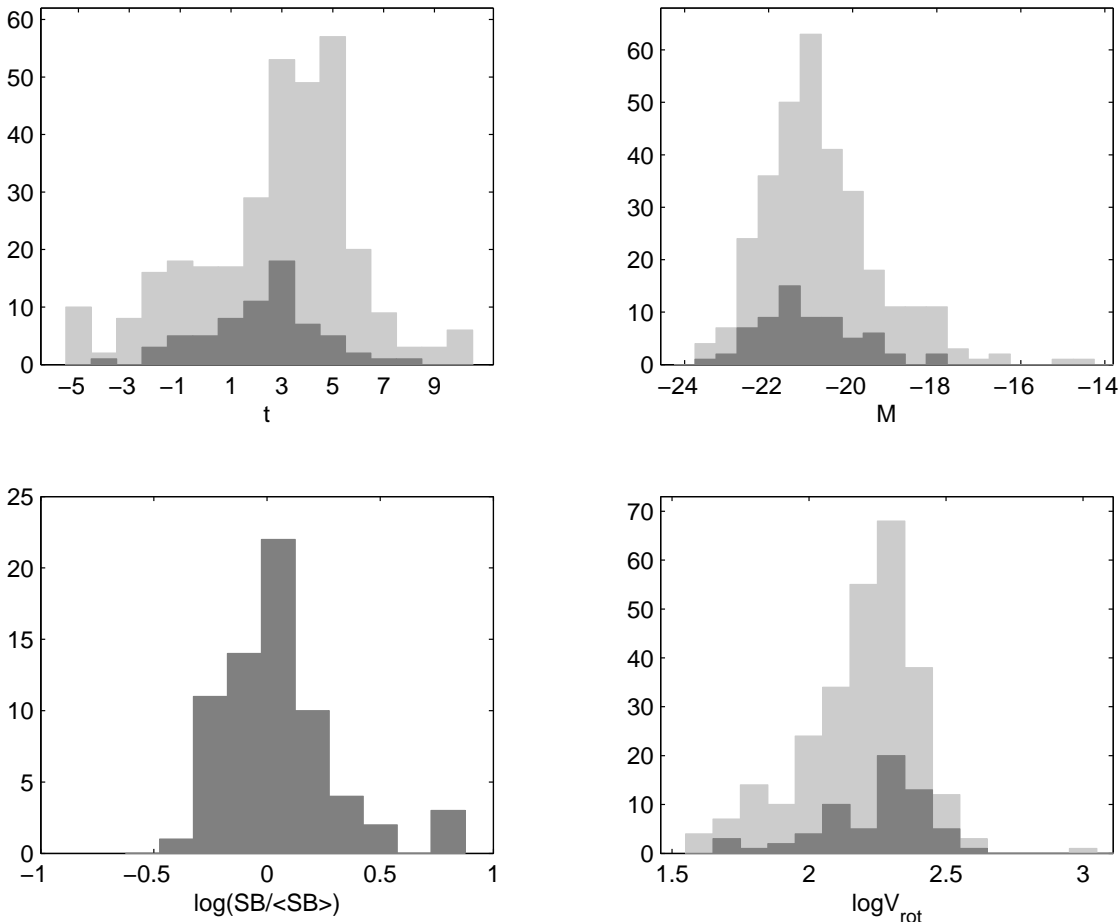


FIG. 1: Distributions of the galaxies in morphological type t , absolute B -band magnitude M , logarithm of the surface density normalized by the mean surface density for the corresponding morphological type, and the logarithm of the rotational velocity, V_{rot} . The light gray histograms show the distributions for all galaxies of catalog [10] with estimated M_{mol} values, while the dark gray histograms are for galaxies in our sample, that is a predominance of molecular gas.

high frequency of occurrences of bars and of nuclear activity (the latter was taken from the catalog [14]). This may be indirectly associated with the concentration of a gas toward galactic centers. The existence of a possible correlation between the abundance of molecular gas and the level of nuclear activity was earlier pointed out in [15].

Thus, galaxies with high M_{mol}/M_{HI} ratios do not differ significantly from other galaxies in their photometric properties, morphological properties, or rotational velocities. However, the question remains open as to what extent the abundance of atomic and molecular gas in such galaxies is really anomalous.

2.2. HI and H_2 Abundances in the Sample Galaxies

A high M_{mol}/M_{HI} ratio could be due to either a high abundance of molecular gas or a reduced mass HI in the galaxy. Let us now compare the

TABLE 2: Percentage of barred galaxies and galaxies with active nuclei (according to [14]) for (1) all objects of CISM [10], (2) galaxies of CISM [10] with molecular-hydrogen mass estimates, and (3) the galaxies of our sample with high relative abundances of molecular gas.

Sample	Bar	Active nucleus	N
1	35.3 ± 0.8	7.7 ± 0.2	1916
2	53.3 ± 3.0	15.8 ± 0.9	317
3	56.7 ± 6.9	22.4 ± 2.7	66

galaxies in our sample with $M_{mol}/M_{HI} > 2$ and all the CISM galaxies of the corresponding morphological types. The left-hand panel in Fig. 2 shows the distribution of the sample galaxies in $lg(\sigma_{mol}/\langle\sigma_{mol}\rangle)$, where $\sigma_{mol} = M_{mol}/D_{25}^2$ is the surface density of the molecular gas within the optical radius, and $\langle\sigma_{mol}\rangle$ is the mean σ_{mol} for all galaxies of the same morphological type with known masses M_{mol} . The right-hand panel in

Fig. 2 shows a similar comparison of the surface density of neutral hydrogen, σ_{HI} . The mean σ_{mol} for the sample galaxies is higher by $\Delta \lg(\sigma_{mol}/\langle\sigma_{mol}\rangle) \approx 0.5$ compared to the average value for all galaxies of the corresponding type. The HI abundance in the sample galaxies is characterized by an asymmetric shape of the distribution of σ_{HI} (note the more gently sloping "wing" for galaxies with strong deficiencies of neutral hydrogen), although the mean σ_{HI} does not differ strongly from the value $\langle\sigma_{HI}\rangle$ for all galaxies of the same morphological type. If we select galaxies with the lowest HI abundances, with surface densities σ_{HI} less than half the mean value, we will find that their mean $\lg(\sigma_{mol}/\langle\sigma_{mol}\rangle)$ is also higher than zero, indicating that, in this case too, we are dealing with an excess of molecular gas. Thus, galaxies with high M_{mol}/M_{HI} ratios really possess high H_2 abundances, rather than having lost their HI as a result of, e.g., its being swept out from the galaxy as a more tenuous component of the interstellar medium.

2.3. Total Gas Mass in the Disks of the Sample Galaxies

We now compare the total gas contents of the galaxies using the relation between the gas mass and the specific angular momentum of the disk, which is characterized by the product of the rotational velocity V_{rot} and radius R of the disk. As the disk radius, we used either the photometric (isophotal) radius R_{25} or the photometric radial disk scale R_0 (in linear units). The relation between the mass of gas and $V_{rot}R$ is obeyed by most of the Sb — Ir galaxies with various brightnesses, both single objects and galaxies with close companions [16], [17] (see also references therein). Although this relation has a physical basis, and follows from the fact that the gas surface densities in most of the galaxies are (on average) close to the threshold density for local Jeans instability, or proportional to this density, here we treat it as a purely empirical relation.

Figure 3 (left, top and bottom) shows the dependence of the mass of atomic gas M_{HI} on the specific angular momentum. All set of CISM galaxies and galaxies from our sample are shown by filled and open circles, respectively. Most of the sample galaxies display HI deficits, which are especially strong among galaxies with relatively low angular momenta. The situation changes radically if instead of M_{HI} we plot the total mass of atomic and molecular gas (including helium) $M_{gas} = 1.4(M_{HI} + M_{mol})$ on the vertical axis (Fig. 3, top right). In this plot, the sample galaxies come closer to the universal relation. Only a few systems fall away from the overall relation because they possess unusually high masses of gas.

Their M_{mol} values are apparently overestimated (see the next section). Thus, the total gas masses for most of the galaxies with anomalously high molecular-gas abundances are consistent with the angular momenta of the galaxies. Hence, the excess H_2 in such galaxies is not neither due to excess "portions" of molecular gas that have come to the galaxy disk, e.g., via the accretion of cold clouds, nor due to overestimates of the H_2 abundances, but instead it is caused by the transition of most of the interstellar hydrogen into the molecular state.

This conclusion remains unchanged if the radial photometric disk scale R_0 is used instead of the optical radius (lower panel of Fig. 3). Note that unlike the isophotal radius, R_0 is not sensitive to differences between the surface brightnesses of the disks of the galaxies compared.

3. POSSIBLE ORIGINS OF HIGH M_{mol}/M_{HI} RATIOS

Let us now list the main reasons that can lead to high estimates of the relative mass of molecular gas.

1. The actual conversion factors for some galaxies may be much lower than the adopted value.
2. This is the effect of the galaxy environment (accretion of large masses of molecular gas onto the disk, or the displacement inward of very cold, difficult to detect, molecular gas from the disk periphery due to interactions between galaxies [18]).
3. An anomalously high content of dust, which serves as a catalyst of the formation of molecules and prevents the dissociation of molecules by the UV radiation of stars.
4. Longer lifetimes of the gas in molecular form compared to most galaxies (e.g., a low star-formation rate per unit mass of molecular gas).
5. Higher gas pressure in regions where it is mainly concentrated, which stimulates the transition of HI into H_2 .

Bellow we analyze each of the above possibilities one-by-one as applied to our sample of galaxies with high M_{mol}/M_{HI} ratios.

3.1. Conversion Factor

The conversion factor X may be higher for galaxies with relatively high heavy-element abundances [1]. Metallicity of gas is usually associated with a high total luminosity L of a galaxy. Since

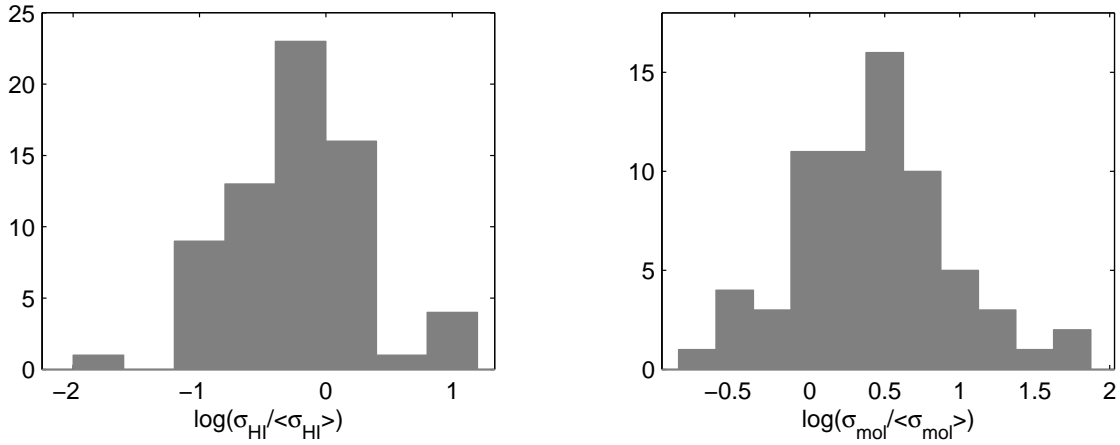


FIG. 2: Histograms of HI and the molecular-gas surface density normalized to the mean values for the corresponding morphological types for the galaxies of the sample studied.

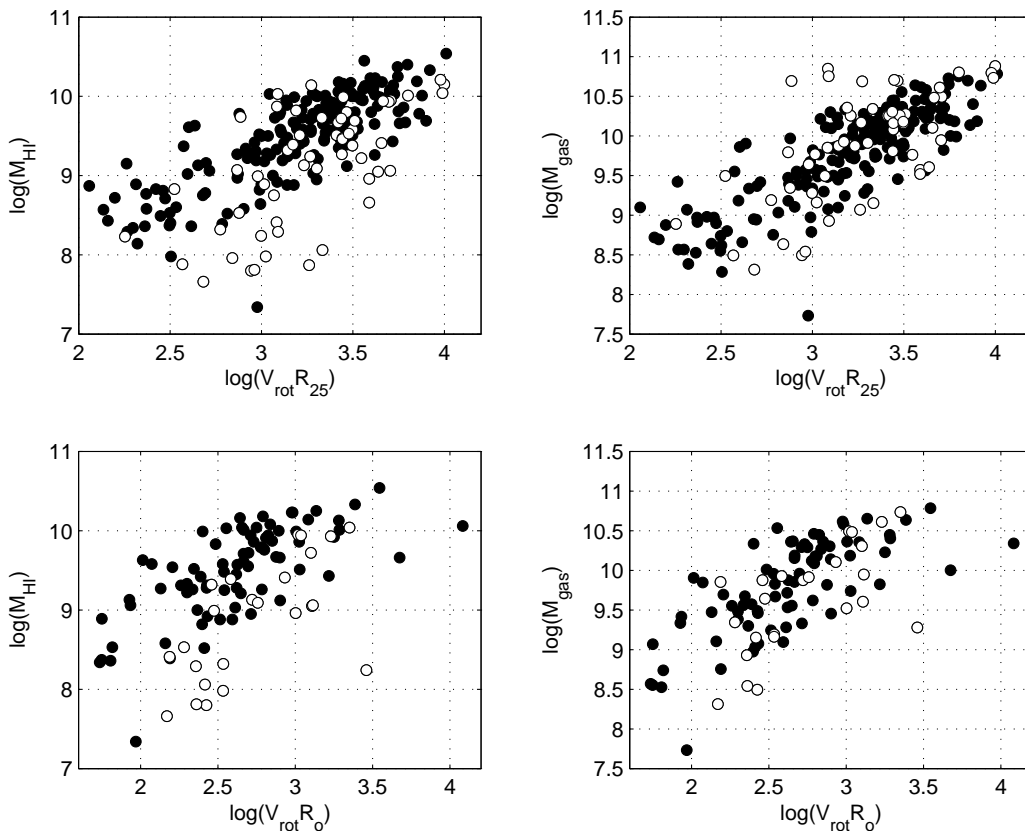


FIG. 3: Mass of atomic gas (left) and total mass of gas (right) as a function of specific angular momentum defined as $V_{rot}R_{25}$ (top) or $V_{rot}R_0$ (bottom) for galaxies of the sample considered (open circles) and for all galaxies of catalog [10] for which the corresponding estimates are available (filled circles). R_{25} and R_0 are photometric radius and a radial scale length of a disk.

the galaxies in our sample are not characterized by very high luminosities (Fig. 1), this explanation is not appropriate for most of our galaxies.

However, some of our sample galaxies may indeed have anomalously low X values. Grounds for this possibility are provided by the fact that the estimated total gas mass M_{gas} (including he-

lium) derived for the adopted X is unrealistically high — comparable to the total mass of the galaxy M_{tot} within its optical boundaries. It is obvious that M_{tot} must exceed the total mass of the disk (not to mention the mass of its gaseous component) if to take into account the masses of the dark halo and bulge. Figure 4 compares the total

gas mass with indicative mass $M_{tot} = V_{rot}^2 D_{25} / 2G$ (in solar units), which is approximately equal to a total mass of a galaxy within D_{25} , for all the CISM galaxies with available estimates of V_{rot} and D_{25} . For galaxies located above the slanting line, $M_{gas} > M_{tot}/2$, and the gas masses are very likely to be overestimated. These galaxies make up a small fraction of all the galaxies considered, but about half of these objects belong to our sample of galaxies with a predominance of molecular gas (open circles). The same galaxies also exhibit a gas excess in the diagrams shown in Fig. 3, supporting the hypothesis that the conversion factors for these objects may have been strongly overestimated. Note that the exclusion of these galaxies does not alter the conclusions drawn above.

Lower conversion factors may be associated not only with high metallicity of a gas, but also with the specific physical state of the interstellar medium. For example, the conversion factor should be low if molecular gas is concentrated not in virialized clouds, as it is usually assumed, but in a less dense diffuse medium [3], which is quite possible in the case of the densest circumnuclear disks, where both clouds and the more tenuous intercloud gas are molecular. The example of *M64*, which dense molecular circumnuclear disk is observed in ^{12}CO and ^{13}CO lines, shows that diffuse molecular gas not only exists, but may even be responsible for the bulk of the *CO*-line luminosity, and the use of the standard conversion factor yields appreciably an overestimated mass of molecular gas [4].

3.2. Effect of the Environment

The effect of the environment is not the main factor determining the high M_{mol}/M_{HI} ratios for the galaxies in our sample. First, the sample contains only a few strongly interacting systems or galaxies in clusters (Table 3). Second, with few exceptions, dense environments around galaxies are not associated with a sharp increase in M_{mol}/M_{HI} . According to de Mello et al. [19], single galaxies and galaxies located in more crowded environments differ only slightly in terms of M_{mol}/M_{HI} , and the mean M_{mol}/M_{HI} ratio for such galaxies remains less than unity. They report $\langle \lg(M_{mol}/M_{HI}) \rangle = -0.69 \pm 0.59$ and -0.51 ± 0.46 for the the means and standard deviations for the high-density sample and the control sample of isolated galaxies, respectively.

3.3. High Dust Content

Let us now compare the galaxies in terms of the mass of dust they contain, estimated from the far infrared (FIR) radiation of galaxies. Figure 5 (top

left) compares the dust surface density defined as M_{dust}/D_{25}^2 in our sample galaxies with the mean dust density for all CISM galaxies of the given morphological type. It is evident that galaxies with a predominance of molecular gas are, indeed, characterized by a higher mean dust content. However, this is probably due solely to the higher mass of gas in these galaxies, since the distribution of M_{dust}/M_{gas} for our galaxies differs little from that for all the CISM galaxies (Fig. 5, top right). Note that the M_{dust} estimate used here refers to so-called warm dust heated by stars, which emits predominantly in the FIR ($40 \div 120 \mu m$). The mass of dust at very low temperatures, which weakly radiates in this spectral interval, cannot be taken into account rigorously. However, there are no grounds to believe that galaxies with a high content of molecular gas detected in *CO* are also characterized by anomalous amounts of very cool dust. The location of the sample galaxies on a two-color diagram likewise does not indicate high color excesses (Fig. 6). The squares on the diagram show the mean color indices for galaxies of various morphological types [20], which mark out the location of the normal color sequence.

Observations show that the mass of dust in galaxies is most closely related to the mass of molecular gas [21]. Figure 5 shows the $M_{dust} - M_{mol}$ diagram for CISM galaxies. The sample galaxies (open circles) lie on the common relation (lower panel in Fig. 5), confirming that these objects have a "normal" content of dust per unit mass of molecular gas (except for a few galaxies).

3.4. Long Lifetime of Gas in the Molecular State

Molecular gas gives birth to stars whose radiation, in turn, leads to the dissociation of molecules. Therefore, the hypothesis that gas spends a long time in the molecular state resulting in the large M_{mol} is equivalent to suggestion of a low star-formation rate per unit mass of molecular gas. It is worth noting that most of the sample galaxies with high M_{mol}/M_{HI} are not characterized by high star-formation rates, as is testified to by their location in the two-color diagram (Fig. 6). Two objects in the "blue" part of the diagram, marked by crosses, are interacting systems or "mergers" (*MCG 5-32-20* and *MCG 5-29-45*), which appear to be undergoing bursts of star formation. Judging by their color indices, most of the galaxies are characterized by moderate or low star-formation rates. The only galaxy that falls away from the overall dependence due to its high (*B-V*) is *NGC1482*, which is a peculiar lenticular galaxy undergoing a burst of star formation in its central region, and is characterized by an extended region of bright line emission and gas outflow (superwind) [22].

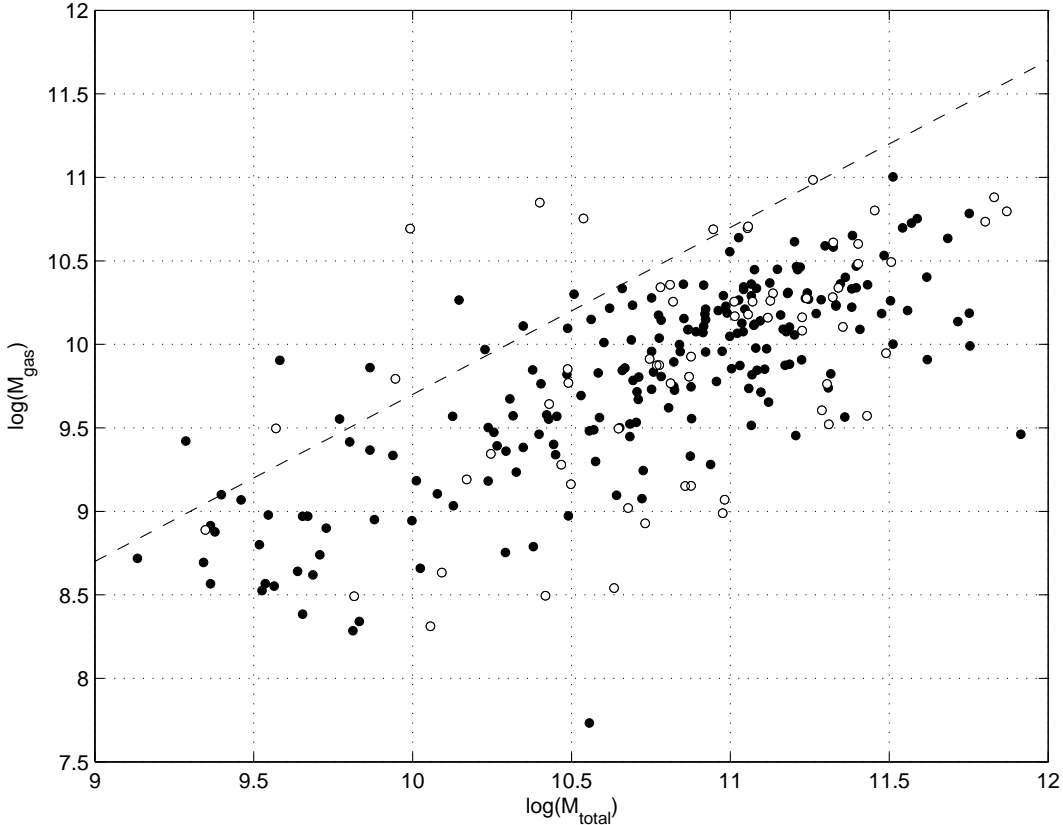


FIG. 4: Estimated total gas mass (including helium) M_{gas} as a function of the total (indicative) mass of the galaxy M_{tot} , within the photometric radius R_{25} . Filled and open circles correspond to CISM [10] galaxies and to galaxies in our sample, respectively. The dashed line corresponds to $M_{\text{gas}} = M_{\text{tot}}/2$. The mass M_{mol} is likely substantially overestimated for galaxies located above this line.

Star formation is a multistage process. If star formation proceeds in a quasi-stationary mode, the mass of gas involved in each stage of the process is proportional to the duration of this stage. In this case, a large amount of molecular gas could be due to a relatively slow formation of gravitationally unstable regions inside molecular clouds (inefficient damping of turbulent motions?) or in the diffuse molecular gas, which evolves on a shorter time scale than the dense clouds.

The current star-formation rate is closely related to the infrared emission by dust L_{FIR} , which absorbs the short-wavelength radiation of stars. To compare the star-formation efficiencies of the galaxies, the left and right panels of Fig. 7 show the relative mass of gas for the CISM galaxies with $L_{\text{FIR}}/M_{\text{gas}}$ and $L_{\text{FIR}}/M_{\text{mol}}$, respectively. The first dependence demonstrates an increase in the star-formation efficiency with an increasing relative H_2 content: the interstellar gas is used up faster in galaxies that are rich in molecular hydrogen than in those with small amounts of H_2 . However, this is true only for the total mass of gas, which in most cases is close to the mass of H_2 . However, as follows from the right-hand plot, the larger molecular fraction of gas, the lower, on

the average, the star-formation rate per unit mass of molecular gas. Consequently, the intensity of the radiation is lower leading to molecular dissociation. This means that, on average, in galaxies dominated by H_2 , the gas should spend more time in the molecular state before it becomes involved in the process of star-formation and dissociation.

On both diagrams, two galaxies deviating strongly from the overall dependence show up conspicuously in the top right corner are *IC860* and *NGC4418*. The anomalously high intensity of their infrared radiation is likely associated with bursts of star formation in these objects [23], [24].

3.5. Excess Pressure of the Interstellar Gas

The pressure of gas is determined mainly by two parameters — the gas surface brightness and the volume density of the disk, which is in good agreement with observations [7], [25], [26]. A high gas pressure appears to be a crucial factor leading to the transformation of neutral (into molecular) hydrogen [6].

A high pressure (density) of gas can be due both to the existence of local regions of com-

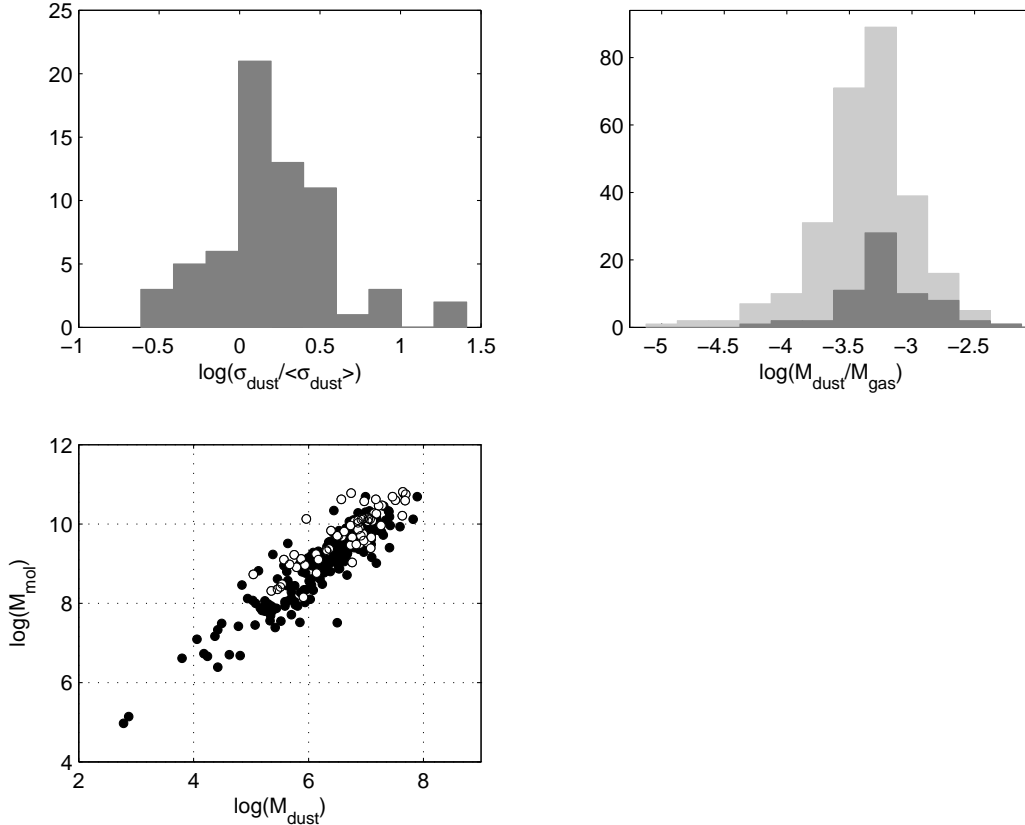


FIG. 5: Dust content in galaxies. Top left: a histogram of the logarithm of the ratio of the surface density of dust to the mean value for the given morphological type according to the CISM catalog [10]; top right: a histogram of the logarithm of the ratio of the mass of dust to the mass of gas (dark gray is for our sample of galaxies, light gray is for all galaxies of the CISM catalog with available M_{mol}); and at the bottom: the dependence of the mass of molecular gas on the mass of dust (filled circles are for all CISM galaxies, while open circles are for galaxies in our sample).

pression (high contrast spiral arms, powerful star-forming regions associated with superclouds) and to a higher density of the stellar disk in the regions containing most of the gas. *M51* is an example of a galaxy with a high relative content of molecular gas in its powerful spiral arms [27]. Giant gaseous complexes are concentrated in the spiral arms, and the gas velocity fields indicate compression of the gas at the front of the shock associated with them. In the absence of strong compressional waves, the gas would first be transformed into molecular form in regions with higher surface density and smaller thicknesses of the gaseous disk. Therefore, the highest gas pressures are expected where gas is concentrated in the inner region of the galaxy. Indeed, about half the gas-rich spiral galaxies (although these do not necessarily show a predominance of H_2 over HI) with available high resolution data on the radial distribution of the CO intensity demonstrate a significant growth of the density of molecular gas toward the center in the inner-disk region [28], [29].

Most of our sample galaxies with $M_{mol}/M_{HI} > 2$ do not show such high-contrast and well-defined

spiral structures as *M51*, but, judging from the Digital Sky Survey images, a circumnuclear region $1 \div 2 \text{ kpc}$ in size can usually be distinguished by its high brightness, which is indicative of intense star formation in the dense central part of a disk. High pressures, and, consequently, a "molecularization" of the gas in the central region of the galaxy could be due to the high surface density of gas combined with the high density of the central part of the stellar disk, whose gravitational field compresses the gas into a thin layer, increasing its volume density.

Unfortunately, data on the radial distribution of the gas are available for only a few of the galaxies in our sample. The best studied example is *M100*, for which a high-resolution radial I_{CO} profile was obtained with the BIMA [28] and Nobeyama Observatory [29] interferometers. Most of the gas in this galaxy is in the molecular state, and is concentrated in an inner region with a diameter of $2 \div 3 \text{ kpc}$ (although the gas also remains mostly molecular at larger distances from the center).

The radial motion of the gas toward the center could be due to both dynamical friction acting on giant molecular clouds and to the interaction of gas

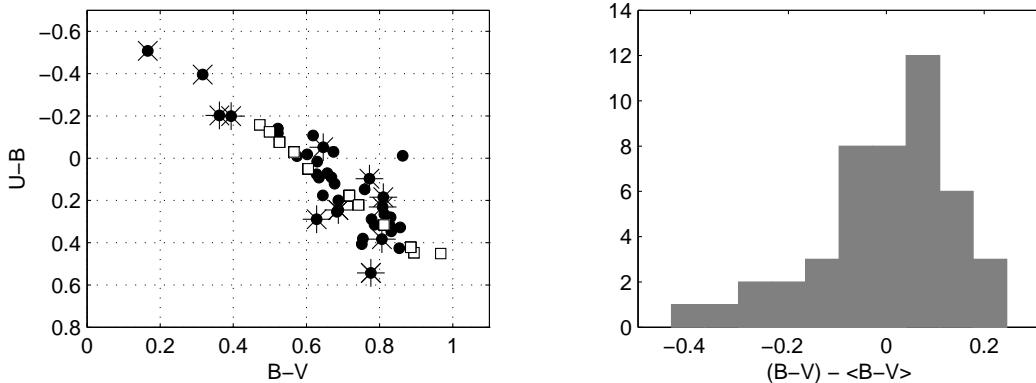


FIG. 6: Left: two-color diagram for the corrected color indices $(U-B) - (B-V)$ (according to the HYPERLEDA database). Filled circles show the galaxies in our sample and squares are for the mean values for galaxies of various morphological types (according to [20]). The X's denote interacting galaxies and the asterisks are for galaxies that belong to clusters. Right: distribution of the galaxies in our sample in the deviation of their $B-V$ color indices from the mean values for the corresponding morphological type).

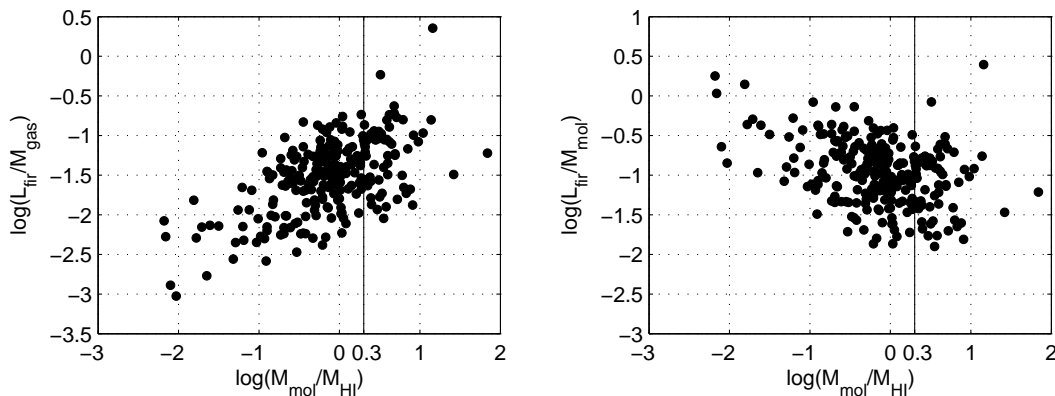


FIG. 7: Dependence of the star-formation efficiency defined as $\log(L_{\text{FIR}}/M_{\text{gas}})$ and as $\log(L_{\text{FIR}}/M_{\text{mol}})$ (right) on the relative content of molecular gas, $\log(M_{\text{mol}}/M_{\text{HI}})$, for CISM galaxies; the vertical line separates the sample galaxies with high fraction of M_{mol} .

with a currently or previously existing bar (recall that more than half of our galaxies have appreciable bars).

4. CONCLUSIONS

Galaxies whose gas is predominantly in molecular form ($M_{\text{mol}}/M_{\text{HI}} > 2$) occur among disk galaxies of all morphological types, although *Sc* — *Sd* types are among these objects. These galaxies differ only slightly from galaxies with lower relative mass of molecular gas in terms of their luminosities, surface brightnesses, rotational velocities, and dust contents per unit mass of gas. At the same time, galaxies that are rich in molecular gas show a tendency to have bars and active nuclei (to be LINERs), providing indirect evidence for a concentration of gas toward the nucleus.

The high $M_{\text{mol}}/M_{\text{HI}}$ ratios in the galaxy sample we have considered is not due to a loss of *HI*

or the acquisition of H_2 , but instead is the result of the transformation of most of the *HI* into H_2 , since the total gas mass, M_{gas} , remains normal and consistent with the specific angular momentum of the disk. However, the M_{mol} values for some of the sample galaxies derived from *CO*-line intensities are probably appreciably overestimated due to the use of a conversion factor that appears to be overestimated.

With only a few exceptions, galaxies with high $M_{\text{mol}}/M_{\text{HI}}$ ratios are characterized by moderate star-formation rates and comparatively high star-formation efficiencies, SFR/M_{gas} . However, the mean star-formation rate per unit mass of molecular gas in these galaxies is appreciably lower compared to galaxies with low $M_{\text{mol}}/M_{\text{HI}}$. This means that, on average, the gas spends more time in molecular form before it becomes atomic again.

As far as the integral properties of our sample galaxies are normal, their high content of molecular gas must be due to specific properties of the

gas in local regions of the disk. The high fraction of molecular gas appears to be due to two interrelated factors. The first of these is a high density (pressure) of the gas due to its concentration in the inner region of the disk (or in spiral arms, if the galaxy possesses a high-contrast spiral structure). In this case, the local dust density should also be higher, facilitating the formation and preservation of molecules. We think that there are no galaxies with a deficit of gas in their central region among those with a predominance of molecular gas. The second possible factor is the long duration of the molecular state of the gas during the chain $HI \rightarrow H_2 \rightarrow$ gravitationally unstable clouds \rightarrow stars. Evidence for this is provided by the systematically lower star-formation rate per unit mass of molecular gas for the sample galaxies. If the gas is concentrated in the inner regions of the galaxy, this delay of its transformation into stars can be logically associated with the high an-

gular velocity of rotation in the inner disk region, which enhances the gravitational stability of the gaseous disk against local perturbations, which, in turn, leads to the accumulation of gas and its subsequent transition into molecular form.

We note, however, that the concentration of molecular gas toward the center of the galaxy is a fairly common (although according to [13], it is less pronounced for galaxies of the latest morphological types). However, a predominance of molecular over atomic gas is a rare phenomenon, implying that a central concentration of a gas is essential, but no means a sufficient condition for such a predominance. To understand better the causes for the transformation of most of HI into H_2 on a galactic scale a more complete picture of gas evolution remains needed.

The work was supported by RFBR grant 04-02-16518.

-
- [1] A. Boselli, J. Lequeux, and G. Gavazzi, *Astron. Astrophys.* **384**, 33 (2002);
- [2] N. Arimoto, Y. Sofue, and T. Tsujimoto, *PASJ*, **48**, 275 (1996);
- [3] D. Downes, P.M. Solomon, *Astrophys. J.* **507**, 615 (1998);
- [4] E. Rosolowsky, L. Blitz, *Astrophys. J.* **623**, 826 (2005);
- [5] B. G. Elmegreen, *Astrophys. J.* **338**, 178 (1989);
- [6] B. G. Elmegreen, *Astrophys. J.* **411**, 170, (1993);
- [7] T. Wong, L. Blitz, *Astrophys. J.* **569**, 157 (2002);
- [8] C. F. McKee, J. P. Ostriker, *Astrophys. J.* **474**, 497 (1977);
- [9] F. Casoli, S. Sauty, M. Gerin, *et al.*, *Astron. Astrophys.* **331**, 451 (1998);
- [10] D. Bettoni, G. Galletta, and S. Garcia-Burillo, *Astron. Astrophys.* **405**,5 (2003);
- [11] HYPERLEDA <http://leda.univ-lyon1.fr/>
- [12] W. E. Baggett, S. M. Baggett, and K. S. J. Anderson, *Astron. J.* **116**, 1626 (1998);
- [13] T. Boker, U. Lisenfeld, and E. Schinnerer, *Astron. Astrophys.* **406**, 87 (2003);
- [14] M.-P. Veron-Cetty, P. Veron, *Astron. Astrophys.* **374**, 92 (2001);
- [15] A. S. Evans, J. M. Mazzarella, *et al.*, *Astrophys. J.* **580**, 749 (2002);
- [16] A. V. Zasov, A. A. Smirnova, *AstL*, **31**, 160 (2005);
- [17] I.D. Karachentsev, V.E. Karachentseva, W.K. Huchtmeier, *et al.*, *Astron. J.* **127**, 2031 (2004);
- [18] D. Pfenniger, F. Combes and L.Martinet *Astron. Astrophys.* **285**, 79 (1994);
- [19] D.F. de Mello, T. Wiklind, and M.A.G. Maia, *Astron. Astrophys.* **381**, 771 (2002);
- [20] R. Buta, S. Mitra, G. de Vaucouleurs, *et al.*, *Astron. J.* **107**, 118 (1994);
- [21] N. A. Devereux, J. S. Young, *Astrophys. J.* **359**, 42 (1990);
- [22] S. Veilleux, D. S.Rupke, *Astrophys. J.* **565L**, 63 (2002);
- [23] I. Kazes, H. Karoji, *et al.*, *Astron. Astrophys.* **197L**, 22 (1988);
- [24] M. Imanishi, K. Nakanishi, N. Kuno, *et al.*, *Astron. J.* **128**, 2037 (2004);
- [25] L. Blitz, E. Rosolowsky, *Astrophys. J.* **612L**, 29 (2004);
- [26] M. H. Heyer, E. Corbelli, *et al.*, *Astrophys. J.* **602**, 723 (2004);
- [27] S. Aalto, S. Huttemeister, *et al.*, *Astrophys. J.* **522**, 165 (1999);
- [28] M. W. Regan, M. D. Thornley, *et al.*, *Astrophys. J.* **561**, 218 (2001);
- [29] K. Sakamoto, S. K. Okumura, *et al.*, *Astrophys. J.* **525**, 691 (1999);

TABLE 3: Galaxies with $M_{mol}/M_{HI} > 2$.

n	Name	Type	Dist. Mpc	R_o	L	D_{25}	$\lg(M_{dust})$	$\lg(M_{HI})$	$\lg(M_{mol})$	$\lg(V_{rot})$	$(U - B)_c$	$(B - V)_c$	Remarks
				Kpc	L_\odot	Kpc	M_\odot	M_\odot	M_\odot	km/s			
1	NGC23	1.2	67	0.57	10.78	1.56	7.14	9.95	10.27	2.45	—	0.72	B
2	NGC142	3.0	113	—	10.64	1.53	7.04	9.73	10.16	2.10	—	—	B
3	NGC695	-2.0	140	—	11.15	1.31	7.64	10.36	10.81	2.45	—	—	
4	NGC828	1.0	78	—	10.88	1.82	7.69	10.15	10.75	2.48	0.32	0.79	
5	NGC972	2.0	23	0.53	10.35	1.34	6.95	9.13	9.75	2.19	0.07	0.66	
6	NGC1022	1.1	19	0.26	9.94	1.16	6.13	8.53	9.24	2.02	0.20	0.69	B
7	NGC1482	-0.9	24	—	9.72	1.19	6.58	8.89	9.68	2.13	-0.01	0.86	
8	UGC2982	5.6	75	—	10.75	1.25	7.28	10.14	10.47	2.32	—	—	B
9	IC2040	-1.0	16	—	9.06	0.81	5.04	8.23	8.73	1.74	—	—	
10	NGC1819	-2.0	63	—	10.49	1.46	6.91	9.51	10.13	2.25	—	—	B
11	NGC2146	2.3	16	—	10.42	1.42	6.80	9.67	10.06	2.30	0.18	0.65	B
12	NGC2775	1.6	19	—	10.46	1.40	6.89	8.66	9.49	2.49	0.32	0.83	
13	NGC3032	-1.9	24	0.30	9.66	1.09	5.79	8.22	8.91	2.27	0.09	0.63	B
14	NGC3147	3.9	44	—	11.02	1.74	7.51	10.21	10.60	2.54	—	0.77	
15	NGC3504	2.1	24	0.40	10.30	1.26	6.52	8.78	9.70	2.25	-0.03	0.67	B
16	NGC3683	5.0	28	0.18	10.17	1.17	6.76	9.32	9.66	2.27	—	—	B
17	NGC3758	2.7	129	—	10.63	1.31	6.89	9.47	9.90	2.43	—	—	
18	NGC3860	2.0	81	—	10.48	1.44	7.01	9.22	9.54	2.41	0.25	0.68	
19	CGCG157 - 46	3.0	96	—	10.16	1.38	6.73	9.03	9.47	—	—	—	
20	NGC3953	4.0	18	0.59	10.63	1.61	7.26	9.41	9.96	2.35	0.12	0.68	B
21	NGC3993	3.1	71	—	10.54	1.53	—	9.80	10.61	2.24	—	—	
22	NGC4064	1.4	15	—	9.81	1.24	5.54	7.96	8.48	1.90	0.09	0.67	B
23	UGC07064	3.3	109	—	10.62	1.44	7.63	9.60	10.21	2.42	-0.02	0.60	B
24	NGC4102	3.0	15	—	9.94	1.14	6.36	8.75	9.37	2.23	—	—	B
25	MCG5 - 29 - 45	3.2	112	—	10.55	1.42	6.74	9.87	10.78	1.97	-0.51	0.17	B, VV
26	NGC4245	0.1	15	0.30	9.65	1.12	5.46	7.80	8.35	2.12	0.43	0.85	B
27	NGC4274	1.7	16	0.63	10.20	1.52	6.32	8.96	9.31	2.37	0.35	0.83	B
28	NGC4298	5.2	18	0.38	10.10	1.18	6.83	8.99	9.48	2.10	—	0.61	V
29	NGC4310	-1.0	15	—	9.05	0.97	5.35	7.88	8.31	1.90	—	—	B
30	NGC4314	1.0	16	-0.06	10.11	1.27	5.67	7.14	8.98	2.33	0.27	0.81	B
31	NGC4321	4.0	24	0.95	11.04	1.72	7.22	9.93	10.46	2.28	-0.05	0.65	B, V
32	NGC4394	2.9	15	0.37	9.91	1.17	5.94	8.56	8.96	2.33	0.19	0.81	B, V
33	NGC4414	5.1	13	0.23	10.14	1.12	6.50	9.39	9.70	2.35	0.10	0.77	V
34	NGC4418	1.0	31	—	9.69	1.13	6.31	8.83	9.34	1.70	—	—	
35	NGC4419	1.1	22	0.13	10.31	1.33	6.39	8.41	9.83	2.05	0.38	0.81	B, V
36	NGC4448	1.8	12	0.04	9.54	0.94	5.51	7.81	8.41	2.32	0.33	0.86	B
37	NGC4450	2.3	30	0.81	10.89	1.64	7.08	9.05	9.39	2.30	—	0.76	V
38	NGC4457	0.5	13	0.49	9.76	1.03	5.57	8.32	9.10	2.04	0.23	0.81	B, V
39	NGC4501	3.3	34	0.89	11.39	1.83	7.68	10.04	10.59	2.46	0.29	0.63	V
40	NGC4548	3.1	8	0.07	10.59	1.10	6.14	8.29	8.76	2.29	0.38	0.75	B
41	NGC4579	2.8	23	0.68	10.82	1.57	6.86	9.06	9.86	2.44	0.41	0.75	B
42	NGC4580	1.6	16	0.15	9.55	0.96	5.91	7.66	8.15	2.02	—	—	B
43	NGC4689	4.7	25	0.66	10.44	1.51	6.62	9.09	9.81	2.09	—	0.60	V
44	NGC4710	-0.8	20	0.24	10.13	1.46	6.17	8.06	9.10	2.17	0.29	0.78	
45	NGC4818	2.0	15	0.41	10.02	1.20	5.87	7.98	9.12	2.12	0.15	0.76	B
46	NGC4848	5.6	104	—	10.83	1.66	6.96	9.27	9.58	2.08	-0.14	0.52	B
47	NGC4858	3.0	137	—	10.30	1.31	6.91	9.05	9.70	—	-0.20	0.36	B, C
48	IC4040	7.2	115	—	10.45	1.44	7.09	9.07	9.66	1.73	-0.20	0.39	B, C
49	NGC4922	-4.4	104	—	10.73	1.58	6.86	9.35	10.03	—	0.54	0.78	VV, C
50	NGC4984	-0.8	17	1.34	9.86	1.18	5.75	8.24	9.22	2.12	0.28	0.83	B
51	IC860	2.4	58	—	10.03	1.19	6.76	7.87	9.03	2.37	—	—	
52	NGC5054	4.1	24	—	10.51	1.53	6.73	9.58	9.96	2.27	0.08	0.63	
53	UGC8399	3.0	107	—	10.37	1.43	6.57	9.74	10.62	1.76	—	—	B
54	MCG5 - 32 - 20	8.0	103	—	10.30	1.25	5.96	9.51	10.13	2.26	-0.40	0.32	VV
55	NGC5187	3.0	105	—	10.36	1.49	6.97	9.99	10.57	2.26	—	—	
56	NGC5653	3.0	54	—	10.62	1.43	7.11	9.69	10.08	2.38	-0.11	0.62	
57	NGC5678	3.3	31	—	10.64	1.48	7.04	9.53	10.13	2.30	—	—	B
58	NGC5676	4.7	34	0.65	10.79	1.58	7.18	9.94	10.26	2.39	-0.01	0.57	
59	NGC5936	3.2	59	0.57	10.59	1.36	7.07	9.63	10.12	2.46	-0.12	0.52	B
60	NGC6000	4.0	30	—	10.31	1.22	6.95	9.82	10.13	2.27	—	—	B
61	NGC6240	0.0	105	—	10.92	1.80	7.46	10.01	10.69	2.30	0.25	0.69	VV
62	NGC6574	3.9	35	—	10.55	1.17	6.86	9.24	10.09	2.40	0.02	0.63	B
63	NGC6951	3.9	24	0.75	10.89	1.39	6.92	9.72	10.11	2.35	—	0.60	B
64	NGC7225	-0.3	68	—	10.51	1.59	7.03	9.38	10.07	2.21	—	—	
65	NGC7770	0.0	62	—	10.17	1.18	—	9.81	10.49	2.59	—	0.47	